Skeletal Radiol (2012) 41:257–271
DOI 10.1007/s00256-011-1146-y

REVIEW ARTICLE

High-resolution 3-T MR neurography of peroneal neuropathy

Avneesh Chhabra · Neda Faridian-Aragh · Majid Chalian · Theodoros Soldatos · Shrey K. Thawait · Eric H. Williams · Gustav Andreisek

Received: 28 December 2010 / Revised: 22 February 2011 / Accepted: 28 February 2011 / Published online: 18 March 2011

Abstract The common peroneal nerve (CPN), a major terminal branch of the sciatic nerve, can be subject to a variety of pathologies, which may affect the nerve at any level from the lumbar plexus to its distal branches. Although the diagnosis of peripheral neuropathy is traditionally based on a patient's clinical findings and electrodiagnostic tests, magnetic resonance neurography (MRN) is gaining an increasing role in the definition of the type, site, and extent of peripheral nerve disorders. Current high-field MR scanners enable high-resolution and excellent soft-tissue contrast imaging of peripheral nerves. In the lower extremities, MR neurography has been employed in the demonstration of the anatomy and pathology of the CPN, as well as in the detection of associated secondary muscle denervation changes. This article reviews the normal appearance of the CPN as well as typical pathologies and abnormal findings at 3.0-T MR neurography of the lower extremity.

Keywords Peroneal nerve · High-resolution MRI · MR neurography

Introduction

The common peroneal nerve (CPN) is a major terminal branch of the sciatic nerve. It can be subject to a variety of pathologies, which may affect the nerve at any level from the lumbar plexus to its distal branches. Although the diagnosis of peripheral neuropathy is traditionally based on the patient's history, clinical findings, and electrodiagnostic tests, we have observed an increasing need for imaging of

Grants AC acknowledges the support from GERRAF (GE), Siemens Medical Solutions, Integra Life Sciences on prospective evaluation of MR neurography techniques.

A. Chhabra (✉) · N. Faridian-Aragh · M. Chalian · T. Soldatos · S. K. Thawait
The Russell H. Morgan Department of Radiology and Radiological Science,
Johns Hopkins Hospital,
601 North Caroline Street, JHOC 3262,
Baltimore, MD 21287, USA
e-mail: achhabr6@jhmi.edu

N. Faridian-Aragh
e-mail: naragh1@jhmi.edu

M. Chalian
e-mail: mchalia1@jhmi.edu

T. Soldatos
e-mail: tsoldat1@jhmi.edu

S. K. Thawait
e-mail: sthawai2@jhmi.edu

E. H. Williams
Department of Plastic Surgery, Johns Hopkins Hospital,
Baltimore, MD, USA
e-mail: williamseb@gmail.com

E. H. Williams
Dellon Institutes for Peripheral Nerve Surgery,
Baltimore, MD, USA

G. Andreisek
Institute for Diagnostic Radiology, Department of Medical Radiology, University Hospital Zurich,
Raemistrasse 100,
8091 Zurich, Switzerland
e-mail: gustav@andreisek.de

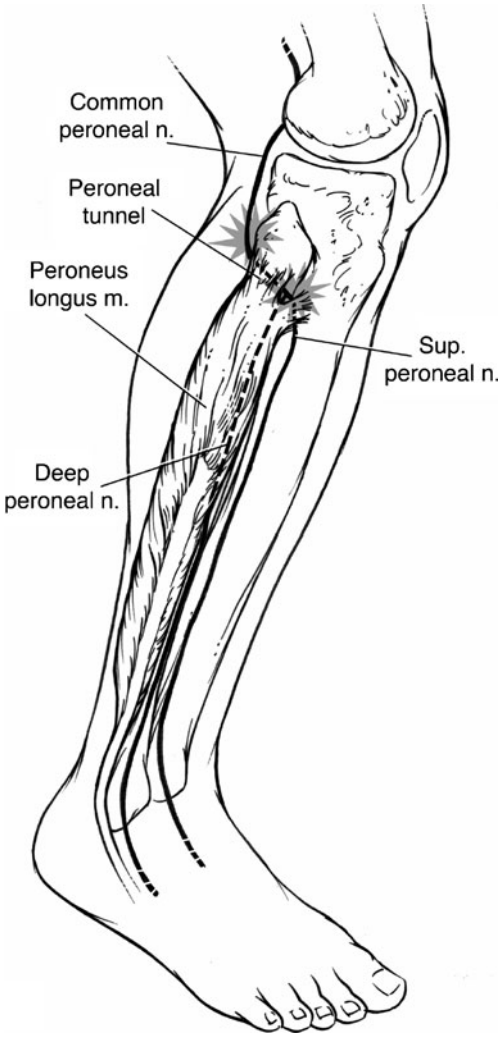

Fig. 1 Anatomical diagram demonstrating sites of entrapment of the peroneal nerve

peripheral nerves in our clinical routine. Common reasons for referrals include the definition of the type, site, and extent of the peripheral nerve disorders. MR imaging has been employed to show the normal anatomy and pathology of the peripheral nerves, as well as to detect associated secondary muscle denervation changes [1–3]. 3.0-T MR scanners enable high-resolution and excellent soft-tissue contrast imaging and at present need to be considered state-of-the-art for the imaging of relatively small anatomic structures such as peripheral nerves. High-resolution MR imaging of nerves is referred to as MR neurography (MRN) by some authors [4]. Literature is sparse with regard to imaging of the CPN. There are some case reports describing the role of ultrasound (US) and some articles describing the use of magnetic resonance (MR) imaging in depicting mass lesions of the CPN, including ganglion cysts [5–11]. However these occasional reports and articles do not provide a comprehensive overview on CPN pathologies, nor do they include current magnetic resonance (MR) imaging techniques such as the use of 3.0-T MR scanners. The aim of this article is to provide a comprehensive review of the normal appearance of the CPN, as well as of typical pathologies and abnormal findings at 3.0-T MRN of the lower extremity.

Normal anatomy and potentials sites of compressive injuries

The mixed motor and sensory sciatic nerve originates from the L4-S2 nerve roots of the LS plexus and is composed of tibial and common peroneal nerve components, which are enclosed in a common nerve sheath. The nerve leaves the pelvis via the greater sciatic notch, coursing beneath the

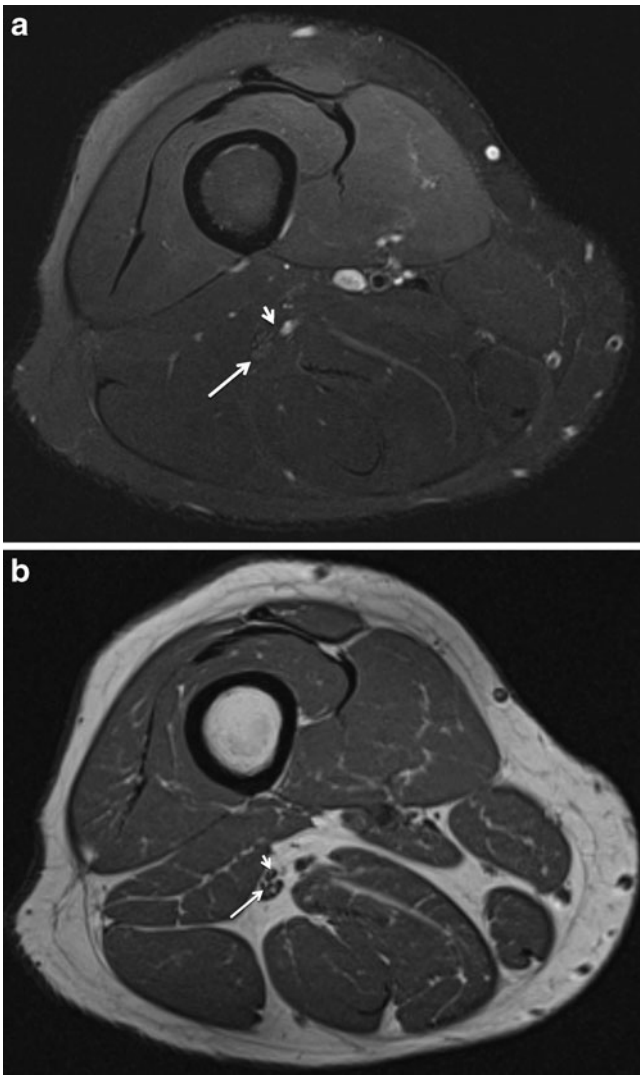

Fig. 2 Normal MRN appearance. Axial T2 SPAIR (**a**) and T1W (**b**) images through the superior aspect of the popliteal fossa shows normal intermediate fascicular appearance of the tibial (*small arrow*) and common peroneal (*large arrow*) components of the sciatic nerve

Table 1 3-T MRN examination protocol for the evaluation of common peroneal neuropathy. *MR* magnetic resonance, *TSE* turbo spin echo, *STIR* short tau inversion recovery, *SPAIR* spectral adiabatic inversion recovery, *3D DW-PSIF* three-dimensional diffusion-weighted reversed fast imaging with steady-state precession (fat-suppressed sequence with a diffusion moment- b value of 80–90 s/mm^2), sampling perfection with application optimized contrasts using varying flip angle evolutions, siemens, erlangen, Germany. Field of view (generally 5 cm above and 15 cm below the knee joint line) is presented in cm, slice thickness in mm, in plane resolution in mm, and TR/TE in ms. *TF* turbo factor, *PD* proton density

MR sequence	FOV	In plane resolution	Slice thickness	TR/TE/TF
Axial T1 TSE	20–22	0.6	3	550/7.9/3
Axial T2 SPAIR TSE	20–22	0.6	3	2840/67/19
Coronal PD	20–26	0.6	3	4100/37/11
3D SPAIR SPACE	20–26	1.0	Isotropic (1 mm)	1020/91/119
Sagittal T2 SPACE	20–26	1.0	Isotropic (1 mm)	1300/87/71
3D DW-PSIF	20–26	0.9	Isotropic (0.9 mm)	10/5/7

piriformis muscle. The CPN and tibial nerve (TN) remain as separate components of the sciatic nerve throughout their course in the thigh without intermingling of their fascicles. The adductor magnus, semimembranosus, and semitendinosus muscles and the long head of the biceps femoris are innervated by motor branches arising from the TN components of the sciatic nerve. The only muscle that is innervated by the CPN components of the sciatic nerve above the knee is the short head of the biceps femoris. In the distal thigh, the sciatic nerve separates into the CPN and TN [12]. The CPN (L4-S1 nerve roots) descends obliquely along the lateral side of the popliteal fossa, posterior to the short head of the biceps femoris muscle and subsequently lateral and superficial to the lateral head of the gastrocne-

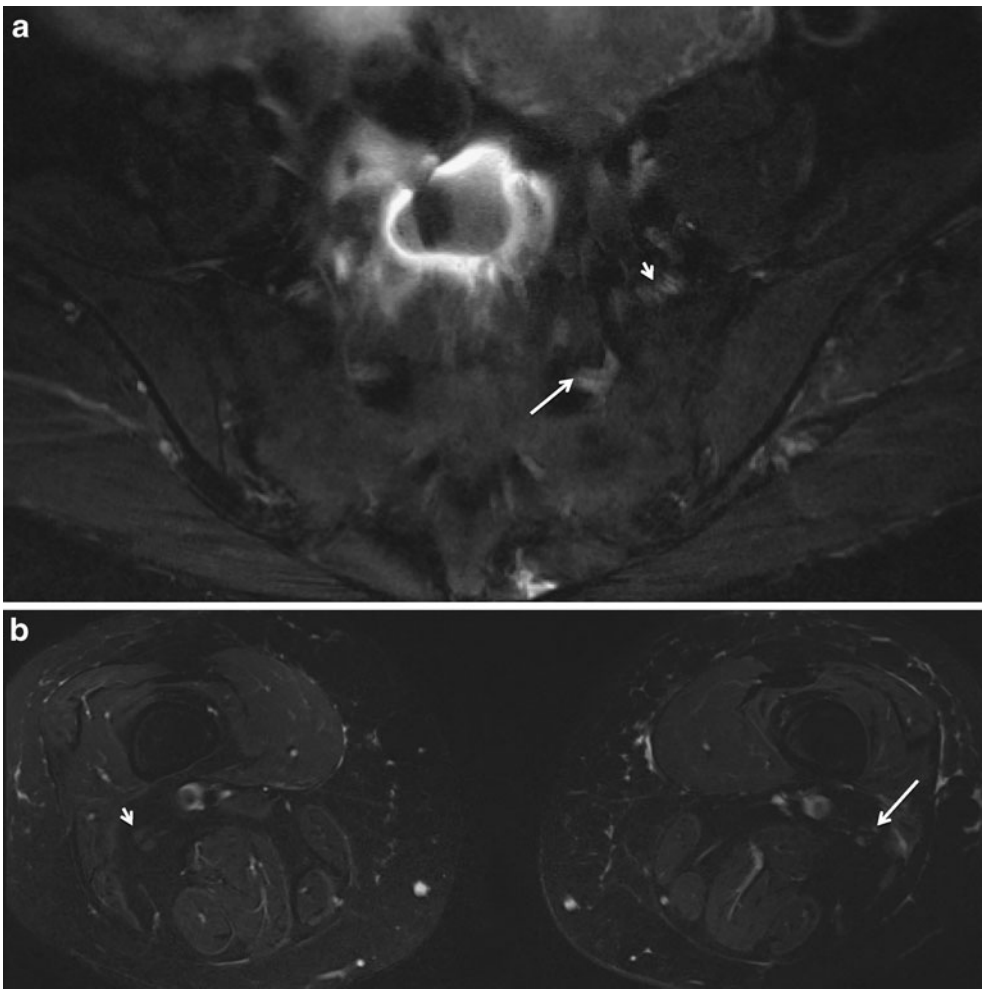

Fig. 3 Lumbar plexopathy with foot drop. Axial T2 SPAIR images through the lumbosacral region (**a**) and distal thighs (**b**) in a 50-year-old woman, status post recent lumbar spine surgery and left foot drop. Notice abnormal T2 hyperintensity and mild asymmetric enlargement of the left L5 (*small arrow*) and S1 (*large arrow*) nerve roots (**a**) adjacent to the susceptibility artifacts from the surgical hardware. The image through the distal thigh show abnormal asymmetric T2 hyperintensity of the left sciatic nerve (*large arrow*) as compared to the right sciatic nerve (*small arrow*)

mius muscle. It gives rise to the lateral cutaneous nerve of the calf, while the medial cutaneous nerve of the calf arises from the TN. The lateral and medial cutaneous nerves of the calf combine distally in the calf to form the sural nerve. More inferiorly, the CPN winds around the neck of the fibula in the peroneal tunnel between the two heads of the peroneus longus muscle and divides into the deep and superficial peroneal branches (Fig. 1). Due to its longer course and relatively fixed position, the CPN is more commonly affected than its tibial counterpart in peripheral compression neuropathies. This is especially seen at the peroneal tunnel, where repeated peroneal muscle contractions related to plantar flexion or ankle inversion actions leads to nerve compression in the tunnel against the fibular neck (Fig. 1) [13, 14]. The CPN and its branches provide motor innervation to the anterior and lateral compartment muscles of the lower leg, as well as sensory innervation to the anterolateral leg and dorsum of the foot. The anatomical configurations of the reinforcement of the deep fascia, adherence of the CPN to the tendon of the biceps femoris and the reinforced fascia as well as soleus and gastrocnemius muscles afford the required protection for the nerve [15, 16]. As the CPN winds around the lateral aspect of the fibular neck, it terminates by dividing into its two superficial and deep branches. The superficial peroneal nerve lies on the anterior intermuscular septum beneath the peroneus longus muscle and supplies both the peroneus longus and brevis muscles. It pierces the crural fascia of the leg, approximately 12 cm above the lateral malleolus, to travel within the subcutaneous tissues as a sensory nerve. At this point, the crural fascia may compress the nerve (the SPN syndrome). The deep peroneal nerve passes proximally through the peroneal compartment before piercing the lateral intermuscular septum and entering into the anterior compartment. It supplies the muscles of the anterior compartment (tibialis anterior, extensor digitorum, extensor hallucis longus, peroneus tertius, and extensor digitorum brevis) [13–17].

Common etiologies and pathologies of CPN neuropathy

CPN neuropathy is the most frequently encountered mononeuropathy in the lower extremity. The CPN may be host to a large variety of diseases, which can be categorized into two large groups. The first group includes systemic diseases, such as systemic inflammations and metabolic disorders such as diabetes amyotrophy, diffuse peripheral polyneuropathies, hyperlipidemia, etc [18–22]. Local conditions such as lumbar plexopathy, sciatic neuropathy, perineural compressive lesions, infections, nerve sheath tumors, and ganglion cysts belong to the second group. Functional anatomical changes, such as habitual leg crossing and repetitive exercise involving inversion and pronation in runners and cyclists, may also cause stretch injury to the CPN. In a large series, the relative distribution of cases of peroneal mononeuropathy were as follows: due to prolonged crossed legs posture (23.1%), surgery (20.3%), idiopathic (16%), weight loss (14.5%), trauma (11.6%), bedridden condition (7.3%), external compression from cast (5.8%), and ganglion cyst at the fibula (1.4%) [18]. Additionally, branches of the CPN may be involved in

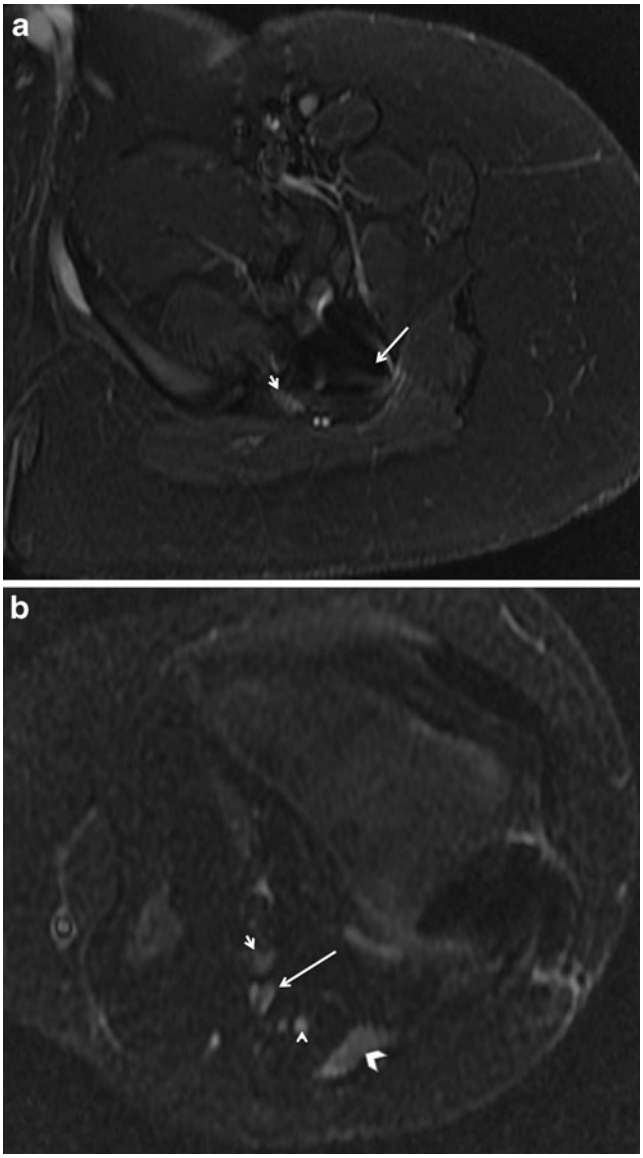

Fig. 4 Sciatic neuropathy with foot drop. Axial T2 SPAIR images through the left hip (**a**) and distal thigh (**b**) in a 9-year-old boy, status post recent left femoral fracture surgical fixation presenting with left foot drop. Notice abnormal T2 hyperintensity of the left sciatic nerve (*small arrow*) adjacent to the susceptibility artifacts from the surgical hardware (*large arrow*). The image through the distal thigh (**b**) shows abnormal T2 hyperintensity of the left TN (*small arrow*), CPN (*large arrow*) as well as lateral cutaneous nerve of the calf (*small arrowhead*). Notice denervation edema like T2 SI in the biceps femoris muscle (*larger arrowhead*)

various compartment syndromes, such as the deep peroneal nerve in the anterior compartment syndrome and the superficial peroneal nerve in the lateral compartment syndrome [13–16].

Clinical findings

Clinical findings depend on the level of the nerve injury or site of entrapment. Peroneal nerve lesions at the level of the LS plexus, thigh and knee usually result in difficulty in ambulation secondary to weakness of the ankle dorsiflexors. Loss of sensation in the cutaneous distribution of the superficial and deep peroneal nerves may also be noted. In traumatic injury, pain secondary to soft-tissue swelling and inflammation may be present. In general, in CPN injury and entrapments, due to the particular arrangement of the fascicles, motor deficits are more commonly seen than the sensory deficits. The motor fascicles are located more medially than the more superficially located lateral sensory fascicles [17].

Tapping of the nerve at the fibular styloid process may produce pain and tingling (Tinel sign) in the sensory distribution of the peroneal nerve. Examination often reveals a variable pattern of weakness, generally worse in the extensor digitorum brevis muscle. In a pure common peroneal neuropathy, plantar flexion and ankle inversion, which are mediated by the tibialis posterior muscle, are generally spared. In lesions around the fibular neck, complete absence of sensation is noted along the anterolateral portion of the leg and dorsum of the foot, while lateral calf sensation (LCN innervation) and action of the short head of the biceps femoris are usually spared [13, 23]. In superficial peroneal nerve syndrome, commonly seen with exercise in runners and cyclists, sensory loss in anterolateral distal leg and the dorsum of the foot is present. In deep peroneal nerve syndrome, the sensory loss is observed over the dorsum of the foot, but the leg is spared. The diagnosis may be confirmed with electromyography (EMG) and nerve conduction studies (NCS). However, these studies are invasive, may be indeterminate at times, and do not reveal information about the extent of the injury, neuroma formation, nerve discontinuity or the cause of entrapment. In clinical practice, infectious, inflammatory and/or metabolic causes, functional neuropathies and compartment syndromes are usually diagnosed by more conventional means, e.g., history, physical exam, and/or electrodiagnostic

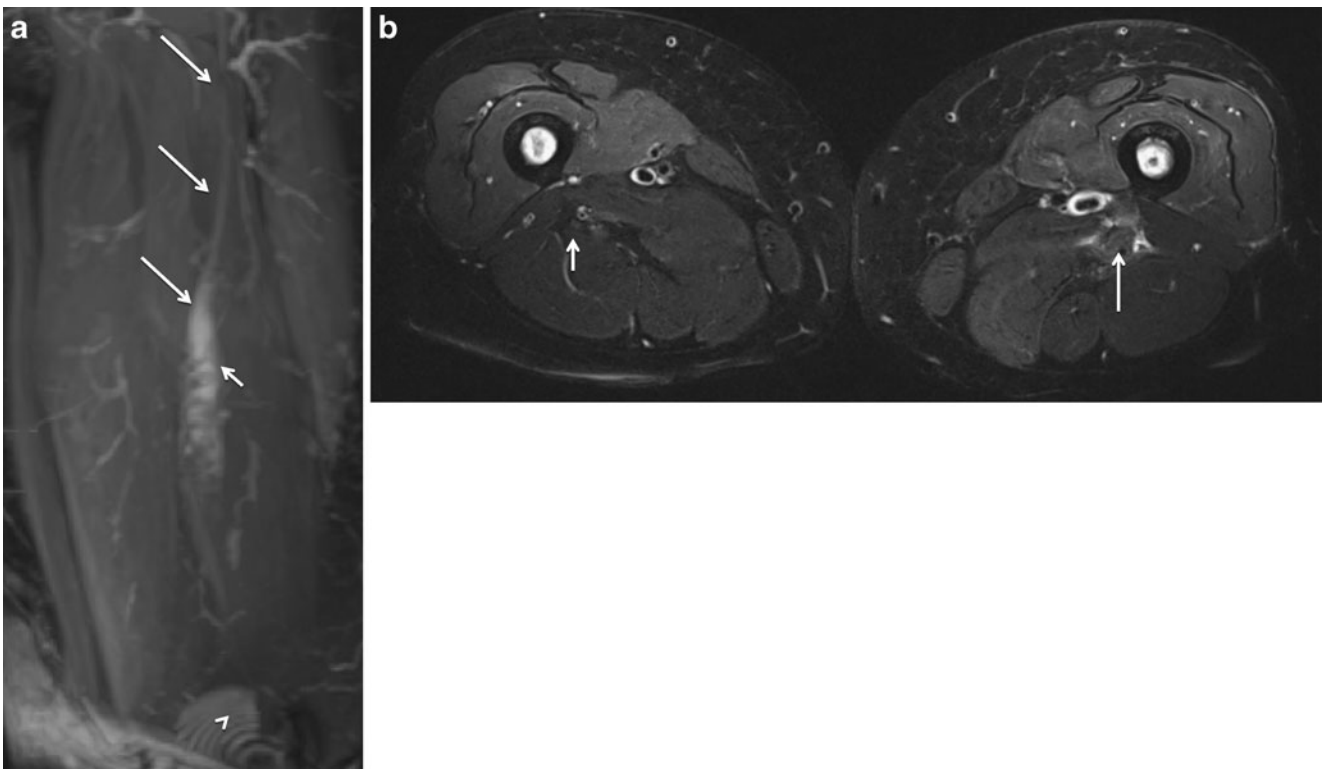

Fig. 5 Sciatic- Neurotmesis. 53-year-old woman, status after recent knee replacement, presenting with foot drop. MIP image from an oblique sagittal reconstructed 3D STIR SPACE image (**a**) through the thigh shows abnormally enlarged and T2 hyperintense neuromatous sciatic nerve (*large arrows*) terminating in an area of hemorrhage (*small arrow*) in keeping with neurotmesis. Notice artifacts from the knee prosthesis (*arrowhead*). Axial T2 SPAIR image through the distal thigh (**b**) confirms the focal hemorrhage (T2 hypointensity) at the site of nerve transection (*large arrow*). Notice normal right sciatic nerve (*small arrow*)

tests. MRN is best used for entrapment neuropathies, assessment of the extent of injury, and mass lesions.

MR imaging evaluation and normal nerve appearance

Due to the continuous technological advancements in MR, this modality has been playing an increasingly important role in the diagnostic algorithm of peripheral nerve diseases [1, 5, 7, 9–11, 24]. MRN can depict subtle T2 signal and fascicular abnormalities and secondary muscle denervation changes and evaluate the sciatic nerve and the deeply situated LS plexus nerve roots [1, 2].

Primary interpretation of sciatic and CPN anatomy and pathology is accomplished on axial T1-weighted (T1W) and T2-weighted (T2W) MR sequences with fat saturation (e.g., SPAIR, spectral adiabatic inversion recovery; Siemens Medical Solutions, Erlangen, Germany). The normal LS plexus and sciatic nerves in pelvis and thighs usually show symmetrical isointense signal intensity (SI) on T1W and minimally hyperintense SI to muscle on fat-saturated T2W MR images. The TN and CPN components of the sciatic nerve can be easily separated on the MR images (Fig. 2). In our experience, the normal TN is always isointense to muscle on all sequences throughout its course from the popliteal fossa to the ankle joint, where it finally divides into the calcaneal, medial planter, and lateral planter nerves. The CPN may show minimally increased T2 signal intensity as it travels obliquely through the popliteal fossa, probably related to magic angle artifacts. The signal intensity returns to isointensity, as it lies beneath the deep fascia of the posterior knee and in the region of the peroneal tunnel. In general, the MR appearance of the nerves should be symmetrical and any asymmetricity in the T2 signal intensity, localized or generalized increase in nerve size, epineurial disruption or thickening and course deviation or change in fascicular morphology (fascicular enlargement, disruption or effacement) points to an abnormality in the nerve. In cases of suspected tumors and the post-surgical cases, as well as the diffuse peripheral nerve lesions such as infections and inflammations, intravenous contrast medium may be used to characterize the lesions. Contrast medium helps in differentiation of post-traumatic neuromas, which usually do not enhance, versus the peripheral nerve sheath tumors, which usually do enhance [1]. However, contrast is usually not helpful in routine cases of traumatic or entrapment neuropathies. The authors do not routinely use contrast for these routine MRN exams at their institute.

Recently, three-dimensional pulse sequences such as 3D STIR SPACE, 3D SPAIR SPACE, and 3D T2 SPACE (3D = three-dimensional, STIR = short tau inversion recovery, SPACE = sampling perfection with application optimized contrasts with varying flip-angle evolutions) have been introduced on 3-T scanners. These sequences exhibit a spin echo-type image contrast and allow isotropic imaging as well as multiplanar (MPR) and curved planar reconstructions (CPR) [25]. Another recent development is a hybrid sequence with low diffusion weighting (b-80-90 s/mm^2) and steady-state nature, 3D DW PSIF (DW = diffusion-weighted, PSIF = reversed fast imaging with steady state precession), an MR sequence that enables excellent suppression of adjacent vessels and creation of nerve-selective images [26]. The use of dedicated workstations with MPR, CPR, and maximum intensity projection (MIP) capability is recommended to reformat the sciatic nerve, CPN and their branches, along the long nerve axis. Although, inline

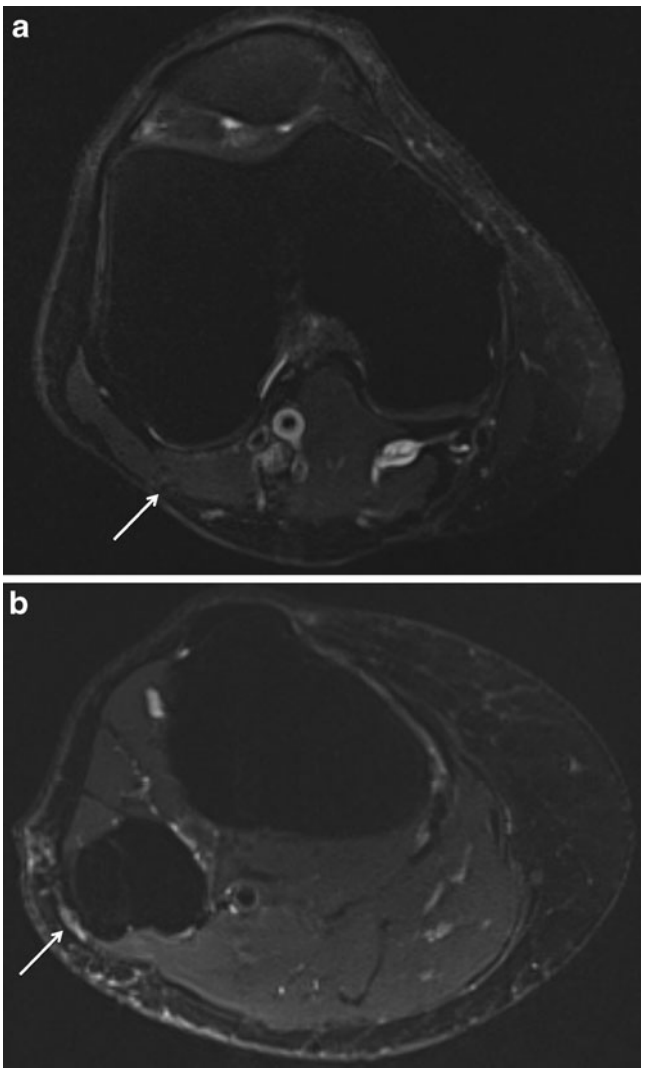

Fig. 6 CPN- Neurapraxia. Axial T2 SPAIR images through the right leg at the level of the popliteal fossa and the fibular head in a 53-year-old woman, status post recent exertion (snow shoveling) presenting with acute right foot drop. There is normal T2 SI on the superior image (**a**) and abnormal T2 hyperintensity of the right CPN at the fibular tunnel (**b**) (*arrows*). The patient improved over a few weeks

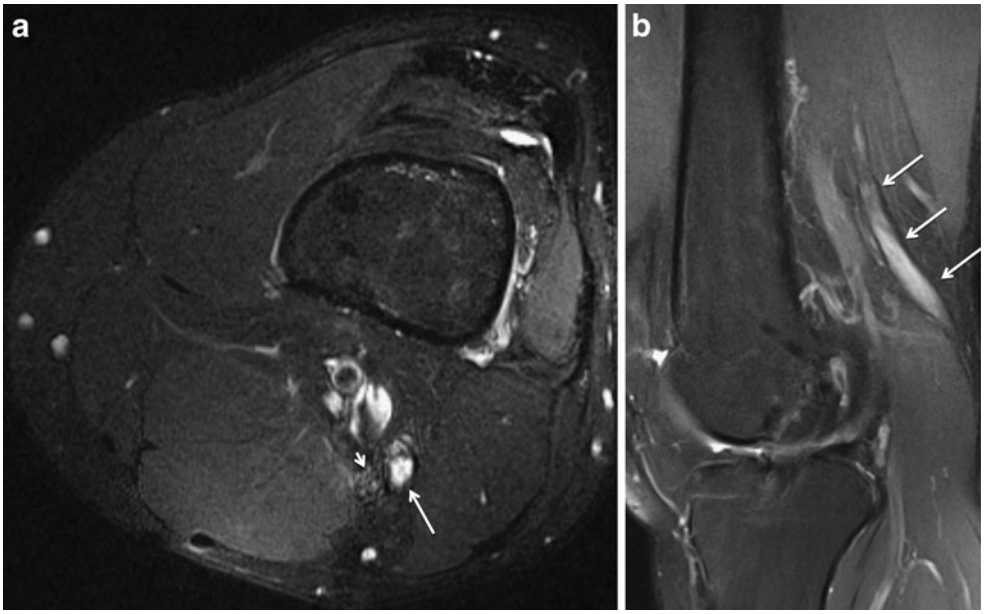

Fig. 7 CPN- Axonotmesis. 22-year-old man, status post previous rotational injury, anterior cruciate ligament disruption and posterolateral corner injury. The patient presented with partial foot drop and pain along peroneal nerve distribution a few months following the ACL reconstruction. Axial T2 SPAIR image (**a**) through the superior aspect of the popliteal fossa shows mildly T2 hyperintense TN (*small arrow*) in keeping with mild neuropathy. Notice fascicular disruption with intact epineurium and abnormal fluid-like T2 hyperintensity of the enlarged CPN (*large arrow*). Sagittal reconstruction from the 3D STIR SPACE image (**b**) confirms the neuroma in continuity involving the CPN (*large arrows*)

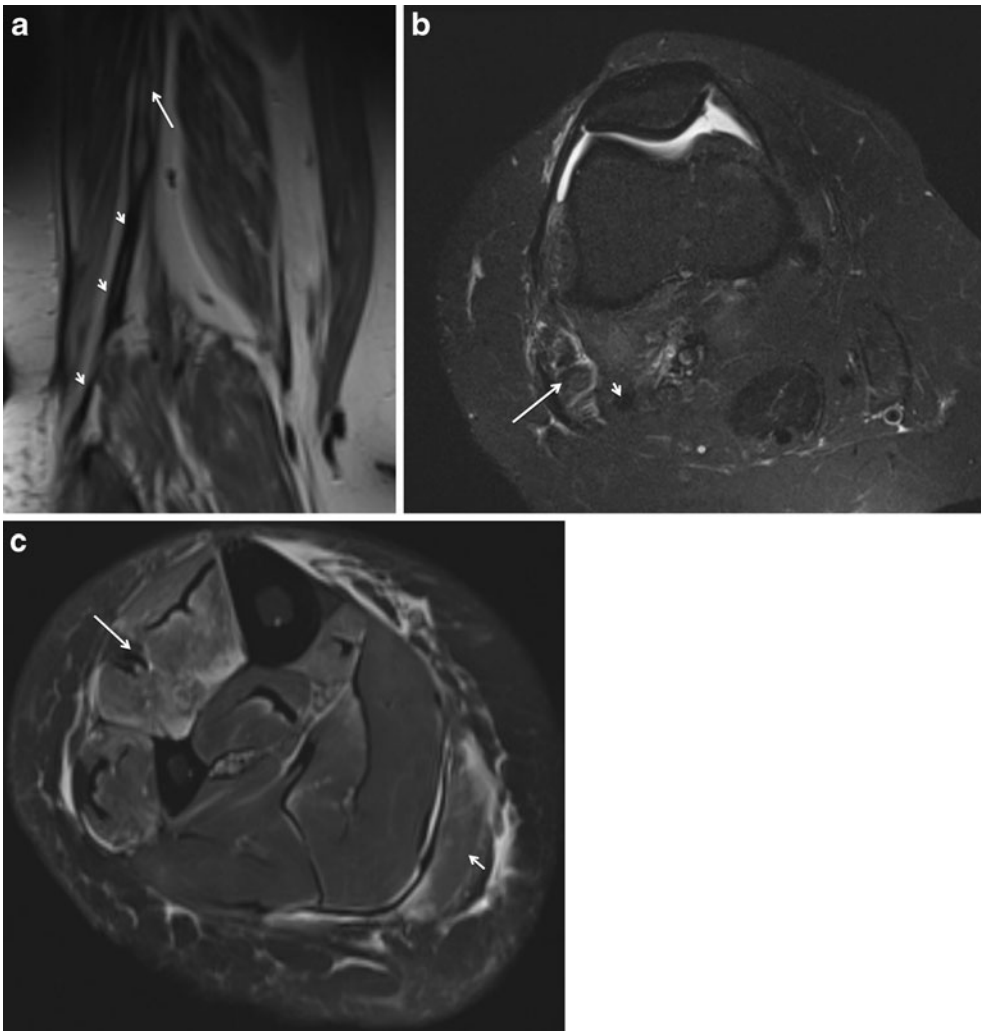

Fig. 8 CPN- Neurotmesis. 42-year-old woman, status after previous knee injury with foot drop. Coronal reconstructed 3D non-fat-saturated T2 SPACE image (**a**) through the leg shows abnormally enlarged and T2 hyperintense CPN (*large arrow*) terminating in an area of fibrosis (*small arrows*) in keeping with neurotmesis. Sequential axial T2 SPAIR images through the popliteal fossa and the proximal calf (**b**, **c**) confirm the fibrosed T2 hypointense CPN (*small arrow* in **b**) and biceps femoris (*large arrow* in **b**) and extensor compartment denervation changes (*large arrow* in **c**). Mild non-specific edema of the gastrocnemius muscle was also noted (*small arrow*)

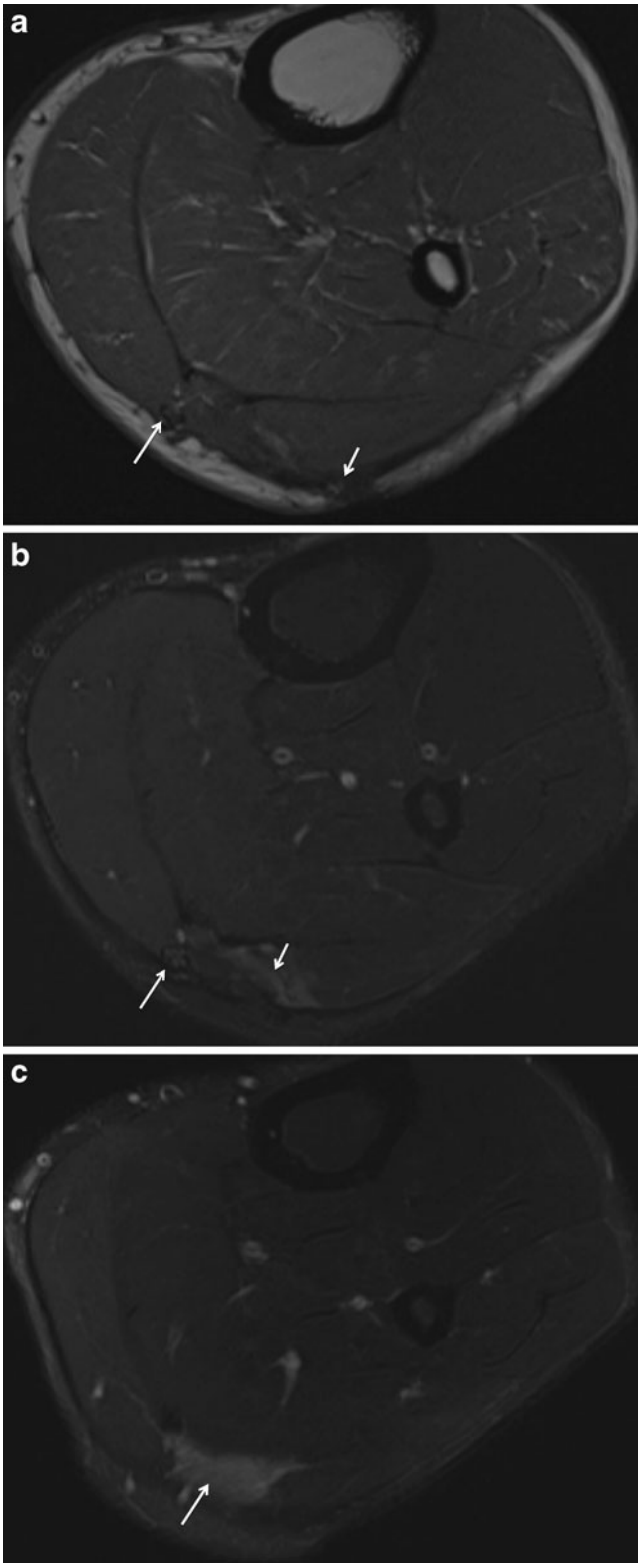

◀ **Fig. 9** Sural nerve neurotmesis. 30-year-old man, status after recent dog bite and skin laceration in posterior calf, presenting with shooting pain along the sural nerve distribution. Axial T1W (**a**) and T2W SPAIR (**b**) images through the proximal calf shows abnormally enlarged neuromatous medial cutaneous nerve (MCN) of the calf (*large arrow*) and fibrosis as well as edema in the expected location of the lateral cutaneous nerve (LCN) of the calf (*small arrow*) from direct injury. Notice large defect in the skin and dermis at the expected location of the sural nerve (*arrow* in **c**). Surgery confirmed complete sural nerve and LCN transection

reformatting can be performed during the routine readouts, it can be demanding for the PACS systems. We have noticed that reformatting performed on Siemens software (Leonardo) or other offline software, such as Vitrea (Vital images) or Centricity (GE) yields better reconstructions and superior image resolution.

With 3-T MR imaging, larger regions of the body can be imaged using large fields of view with uniform magnet homogeneity, even in off-center areas. In addition, frequent use of water-selective fat saturation (Dixon) techniques provides more robust fat suppression. It is prudent to protocol the MRN exam following discussions with the referring physicians or based on the available clinical and electrodiagnostic information for optimal imaging of a pre-determined anatomical area. In certain cases, however, this pre-selection of the field of view is not possible, and multiple areas of the body can be quickly screened using T1 and STIR images at a lower spatial resolution. Then, the prospectively determined target area should always be evaluated using high-resolution MRN sequences. Table 1 shows the imaging protocols used in our department for the detection of CPN pathology. A similar protocol can be used for sciatic pathology and LS plexus evaluation. In the authors' experience, the main difference is that 3D SPAIR SPACE works better in the extremities with better SNR, while 3D STIR SPACE works better for the LS plexus with better fat saturation. For image reception, the authors use an eight-channel knee coil (InVivo Corporation, Orlando, FL, USA), or a four-channel phased array flexible surface coil (Siemens Medical Solutions, Erlangen, Germany) depending upon the coverage needed. Although, knee coil provides the best resolution, its field of view is limited to 12–15 cm.

The regional muscle denervation changes of edema-like T2 SI in early stages of nerve entrapment/injury and increasing fatty replacement and atrophy in subacute and chronic stages, serve as useful secondary findings of neuropathy. Involvement of the tibialis anterior and extensor digitorum muscles indicate DPN lesions; SPN lesions involve the peroneus longus/brevis muscles; and the CPN lesions involve both of these muscle groups. L5 lesions, a clinical differential diagnosis of CPN lesion, typically involve the popliteus and posterior tibial muscles as well. More extensive denervation abnormalities are associated with nerve abnormalities of the LS plexus and the sciatic nerve [22]. In general, MRN examination should be tailored to the suspected site of pathology based on clinical and EMG findings.

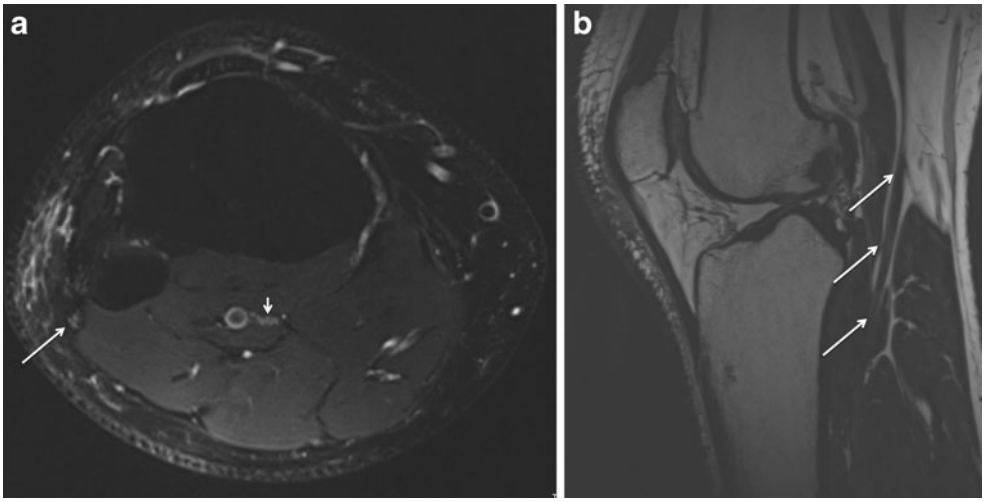

Fig. 10 Double entrapment. 36-year-old man with right leg pain and positive Tinel signs at the peroneal tunnel and posterior upper calf. Axial T2W SPAIR image (**a**) through the upper calf shows abnormal T2 hyperintensity of the TN just proximal to the soleal sling entrapment site (*small arrow*) as well as of the CPN just proximal to the fibular tunnel (*large arrow*). Sagittal reconstruction from 3D T2 SPACE sequence (**b**) shows abnormally flattening of the tibial nerve at the entrapment site (*arrows*)

Fig. 11 Sciatic lymphoma. 67-year-old woman being treated for B-cell lymphoma, presents with right leg pain and foot drop. Axial T2W SPAIR image (**a**) through the distal thighs shows abnormally enlarged neuromatous right sciatic nerve (*large arrow*), diagnosis was confirmed on surgical biopsy. Notice the normal left sciatic nerve (*small arrow*). Post-contrast fat-suppressed coronal T1W image (**b**) shows patchy enhancement in the lesion in keeping with known history of lymphoma (*arrow*)

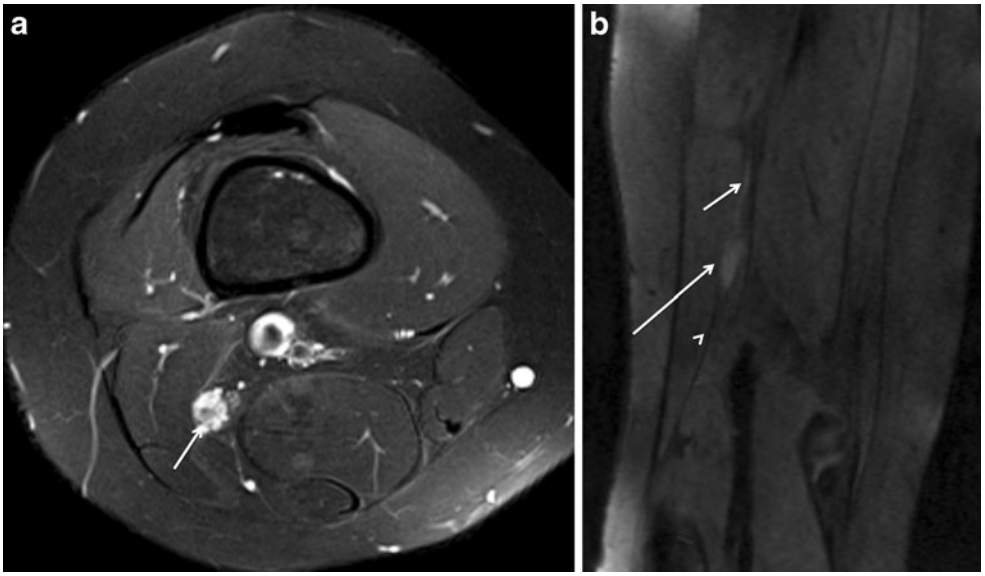

Fig. 12 CPN perineuroma. 13-year-old boy presenting with gradual onset of foot drop over a 6-month period. Axial T2W SPAIR (**a**) image through the distal thigh shows abnormally enlarged neuromatous CPN (*arrow*) and enlarged fascicles in a biopsy proven perineuroma. Coronal 3D DW PSIF image (**b**) shows the full extent of this surgically proven mass lesion (*large arrow*) with proximal enlarged abnormally hyperintense nerve (*small arrow*) and normal distal nerve (*arrowhead*)

Lumbar plexopathy and sciatic neuropathy

Common causes for neuropathies affecting the CPN, which are primarily located above the knee, include lumbar plexopathies, L5 radiculopathy, and sciatic neuropathy [27]. A variety of lesions can involve L4-S1 nerve roots, resulting in lumbar plexopathy, sciatic neuropathy, and

Fig. 13 Schwannomatosis with CPN involvement. 19-year-old man presenting with right leg pain over a 6-month period. Coronal STIR image (**a**) through the leg shows multiple PNSTs involving the CPN (*arrows*) and the TN (*arrowhead*)

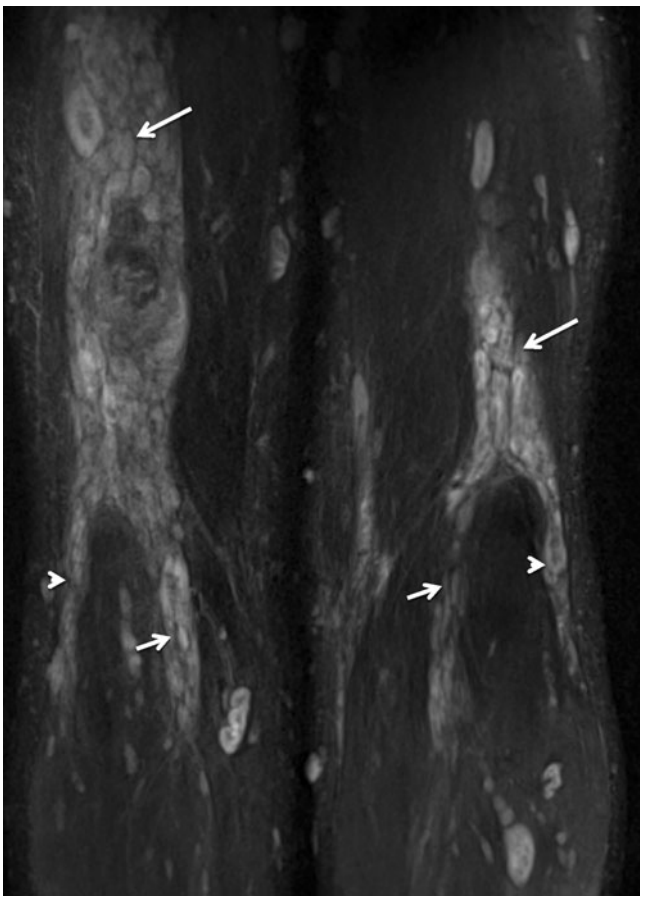

Fig. 14 Neurofibromatosis with CPN involvement. 31-year-old woman presenting with right leg pain. Coronal STIR image through both legs shows numerous PNSTs involving bilateral sciatic nerves (*large arrows*) as well as TN (*small arrows*) and CPN (*arrowheads*)

CPN neuropathy. These lesions include degenerative spondylotic changes, infectious and/or inflammatory etiologies, tumors, trauma, spine surgery, ischemic, and metabolic causes, etc. [19]. On MRN, there may be abnormal T2 hyperintensity, enlargement and/or course deviation of one or multiple nerve roots, based on the site of pathology (Fig. 3). The complication rate of nerve root injury from lumbar disc surgery ranges from 0.7 to 2.2%. Postoperative radicular neuromas must be considered in the differential diagnosis for patients with failed back surgery syndrome [28]. In the latter case, the sciatic nerve and CPN nerve may demonstrate asymmetry of the SI and/or size, as well as an abnormal fascicular pattern. The regional muscle denervation changes may be apparent in the paraspinal region in isolation or together with muscles in multiple compartments of the leg, depending upon the extent and distribution of the injury.

Traumatic neuropathy

Femoral fracture/dislocations and their repairs by surgical fixation may be complicated by sciatic nerve injury and palsy in approximately 4% of cases (Fig. 4) [29]. Iatrogenic sciatic nerve injuries may occur during hip and knee prosthesis placement. Patient typically develops an acute foot drop after surgery (Fig. 5). The CPN may be subject to direct penetrating or blunt trauma. Common scenarios include fibular fracture, knee dislocation, posterolateral corner injury and repair, as well as direct laceration, such as from a dog bite (Figs. 6, 7, 8). The CPN is the most frequently injured peripheral nerve, however, its branches, such as superficial peroneal nerve and lateral cutaneous nerve of the calf may also be injured in isolation (Fig. 9) [11, 30–32]. The superficial peroneal nerve maybe injured by trauma or during surgery, especially around the ankle

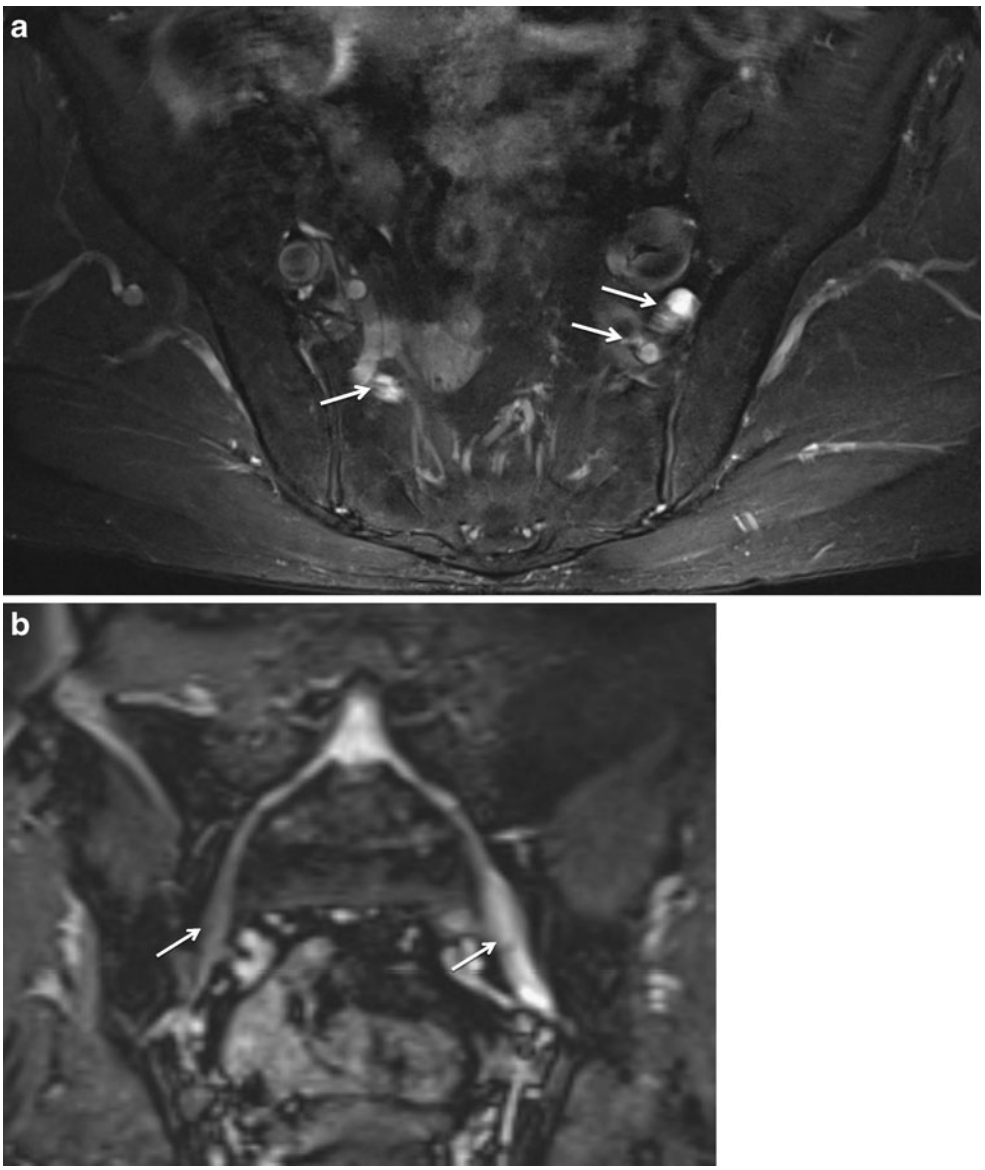

Fig. 15 Idiopathic polyneuropathy with foot drop. 60-year-old man with left leg pain and foot drop. Axial T2W SPAIR image (**a**) shows multifocal lumbosacral plexus enlargement (*arrows*). Coronal reformat from 3D STIR SPACE image (**b**) through the lumbosacral plexus confirms the multifocal diffuse peripheral nerve enlargement (*arrows*) in keeping with EMG diagnosis of multifocal neuropathy. No specific cause could be discerned

[33]. According to the Seddon classification, nerve injuries may be mild (neurapraxia: stretch or ischemic injury, Fig. 6), moderate (axonotmesis: partial discontinuity with or without formation of neuroma in continuity, Fig. 7) or severe (neurotmesis: complete discontinuity, Figs. 5, 8, 9) [1, 2]. Mild-moderate nerve abnormalities on MRN should be differentiated from the nerve discontinuity of severe nerve injury, which requires immediate surgery. MPR using 3D images is particularly helpful in depicting fascicular abnormality, neuroma in continuity and physical nerve discontinuity (Figs. 5, 7, 8). Extensor compartment muscle denervation changes serve as useful secondary signs of nerve abnormality (Figs. 8b, c, 16b). Metal suppression techniques should be used in all current MR imaging protocols for post-surgical patients (e.g., increasing the receiver bandwidth or matrix size, higher echo train length, use of lower TE, use of fast spine echo sequences and avoidance of gradient echo sequences, etc.) to be able to depict the extent of the nerve injury even in patients with extensive metal hardware such as prostheses. Demonstration of any nerve discontinuity (neurotmesis) is an indication for an immediate re-surgery and nerve repair. Nerve regeneration following CPN repair is poor as compared to other peripheral nerves. The surgical outcome can dramatically be improved when tibialis posterior tendon transfer procedures are performed along with CPN repair [34].

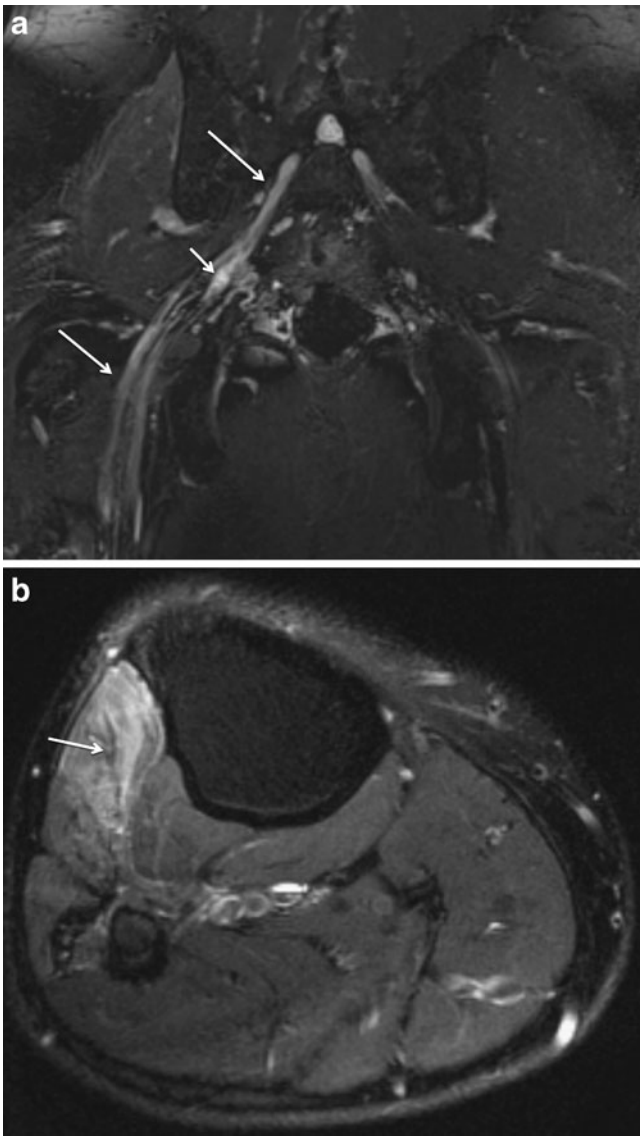

Fig. 16 Amyloid neuropathy with foot drop. 45-year-old white man with right leg pain and foot drop. Coronal reformat from 3D STIR SPACE image (**a**) through the lumbosacral plexus shows diffuse LS plexus and sciatic nerve enlargement (*large arrows*) with enlarged fascicles and multifocal masses (*small arrow*). Biopsy confirmed the diagnosis of amyloid deposition. Axial T2W SPAIR image through the calf (b) confirms the extensor compartment muscle denervation changes (*arrow*)

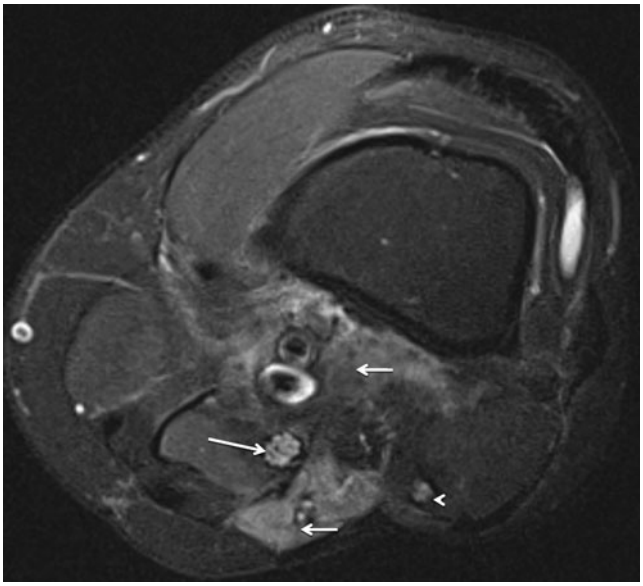

Fig. 17 Post-radiation change. 37-year-old asymptomatic man, status post-surgery and radiation treatment for myxoid liposarcoma. Axial T2W SPAIR image through the distal thigh shows enlarged and T2 hyperintense TN (*large arrow*), CPN (*arrowhead*) and post-treatment changes (*small arrows*)

Entrapment neuropathy

While the CPN may be entrapped at any level along its course, the most common location is within the peroneal tunnel due to the fixed nerve position between the bone and the fascia. The lesions may result from pressure on the nerve at the fibular neck during sleep, from habitual leg crossing, anorexia, or following bariatric surgery (from rapid weight loss). However, nerve compression can also result from space-occupying lesions, including ganglion cysts, large baker cysts, soft-tissue tumors, osteochondromas, and other bony tumors, malunited fractures, tight leg

cast [5, 8, 10, 13, 16, 18, 21, 22, 35–37], post-traumatic hematoma, postsurgical scar [38], and posterior tibial artery aneurysm [5]. The peroneal ganglia have been reported as an important cause of neuropathy. The most widely accepted theory describes the formation of ganglion as a result of the synovial extension along an intra-articular branch of the CPN from the proximal tibiofibular joint [10, 37, 39]. With dynamic pressure changes, these ganglia may vary in size and may involve various branches of the CPN or the sciatic nerve with either anterograde or retrograde extension [37, 39]. In our experience, these ganglia are very rare. Instead, it is much more common to find focal entrapment of the CPN at the fibular tunnel by thickened fascia or perineural fibrosis. The most common location of SPN entrapment is at the segment where it pierces the crural fascia [33]. MRN may directly show the cause and/or the site of entrapment. Typically, an abnormal nerve T2 hyperintensity of the CPN at and just proximal to the compression site, along with nerve flattening at the site of entrapment is seen. Regional muscle denervation changes may be apparent. Less commonly, dual entrapment of the TN at the soleal sling site and CPN at the fibular tunnel may occur, thereby leading to generalized leg weakness, calf and anterolateral leg pain, as well as corresponding positive Tinel sign at the above-mentioned sites [32]. Abnormalities of both TN and CPN should be sought for on these high-resolution examinations (Fig. 10).

Tumor and tumor-like conditions

The CPN may be affected by tumors involving the sciatic nerve, space-occupying lesions adjacent to the sciatic nerve (Fig. 11) or the CPN, or be directly involved by tumors, such as peripheral nerve sheath tumors (PNST), or tumor-like conditions, such as fibrolipomatous hypertrophy, perineuroma (Fig. 12), amyloidoma, inflammatory pseudotumor, etc [6, 12, 40–43]. The PNSTs may occur in isolation or may be associated with schwannomatosis or neurofibromatosis (Figs. 13, 14) [44–46]. These tumors are more frequently benign (benign peripheral nerve sheath tumors; BPNST) [48]. A BPNST may be an incidental finding, or it may present with mild pain or dysesthesia. On the other hand, symptoms of malignant peripheral nerve sheath tumors (malignant peripheral nerve sheath tumors; MPNST) are usually more severe at presentation, with enlarging mass and severe sensory-motor symptoms. MR imaging is the modality of choice for the evaluation of PNSTs, as it can delineate the lesion and define the relationship of the tumor with the surrounding neurovascular tissues and muscles. The usual appearance of a benign tumor is that of ovoid, round, or fusiform mass with well-defined margins. These lesions may involve the sciatic nerve, TN, CPN, or their branches. Several signs, such as target sign, fascicular sign, tail sign, and split fat sign have been described as signs of benignity, but none of them is pathognomonic, as they are rarely present in MPNSTs. On post-contrast images, MPNSTs may show variable or homogenous enhancement.

Diffuse polyneuropathies

Diffuse peripheral polyneuropathies may be idiopathic or may be related to hereditary neuropathies, such as Charcot-Marie-Tooth disease, hereditary motor sensory neuropathy, leprosy, and tumor-like conditions, such as neurofibromatosis, lymphoma, or amyloidosis [2, 42]. Whole-body diffusion-weighted MRI may potentially have a role in the assessment of the full burden of these conditions in the

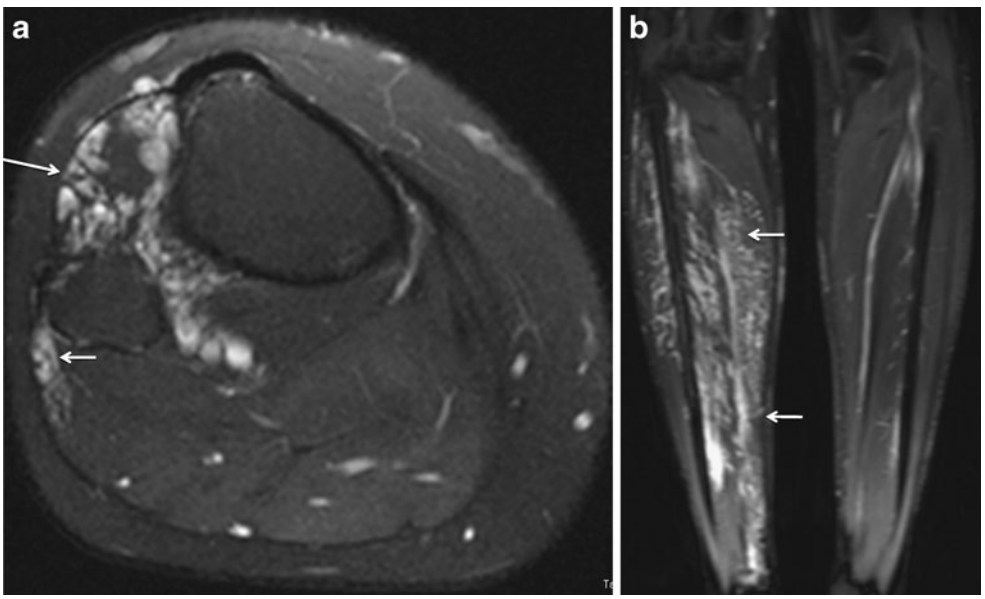

Fig. 18 Venous malformation. 17-year-old female with right leg tingling, burning, and aching pain. Axial STIR image (**a**) through the proximal calf shows a large venous malformation (*large arrow*) encasing the CPN, which is not separately discerned from the abnormal venous structures (*small arrow*). Coronal STIR image of both legs (**b**) shows the full extent of the malformation (*arrows*)

future; however, it is still in experimental stage [48]. In contrast to tumors and tumor-like conditions, which may produce multifocal masses along the course of the enlarged nerve, hereditary and infectious neuropathies usually present as long segments of uniform enlargement and increased T2 signal (Fig. 15) [49]. The enhancement patterns may vary, with the most enhancements seen in cases of chronic inflammatory demyelinating neuropathy and tumor variants [2]. Amyloidosis of the sciatic nerve results in multifocal distribution with epineurial amyloid deposits, endoneurial edema related to vascular amyloid deposition and segmental demyelination resulting from nerve ischemia [50]. MRN shows the full extent of diffuse nerve thickening, abnormal T2 hyperintensity, fascicular enlargement, and multifocal masses. Contrast enhancement is variable. Regional muscle denervation changes may also be apparent, but can be very variable (Fig. 16) [2].

Miscellaneous conditions

Other etiologies for sciatic and CP neuropathy include radiation neuropathy [51, 52] and pathologies in the vicinity of the nerve such as vascular malformations and thrombophlebitis. Peripheral nerves may be injured due to radiation effects in up to 13% of cases treated for extremity sarcomas. Predisposing factors for the development of radiation-induced neuropathy include, the total radiation dose exceeding 60 Gy and dose per fraction greater than 2 Gy [53].

These changes lead to the clinical manifestations of progressive paresthesias and dysaesthesias, paresis, atrophy, and edema. However, it should be remembered that in cases with recent history of radiation, the regional nerve in the radiation field may enlarge and show abnormal increase in T2 signal on MRI, while the patient may be completely asymptomatic (Fig. 17). Hence, to prevent false-positive diagnosis of neuropathy, MR findings should be correlated with clinical findings. Perineural vascular malformations may secondarily affect the nerve by involving the nerve sheath. In these cases, neuropathy cannot only be caused by the vascular malformation, but it can also be induced by the embolization procedures during treatment (Fig. 18) [54]. However, MR-guided embolization may help to reduce the complications rate and to preserve peripheral nerve function [55].

Conclusions

The CPN and its branches can be the host to a variety of pathologies. High-resolution 3.0-T MRN is the imaging modality of choice in cases with a clinical suspicion of CPN neuropathy. It may supplement the information gained from the patient's history, clinical examination, and electrodiagnostic findings by directly demonstrating the site, extent, and type of primary nerve abnormality, surrounding lesions, as well as secondary regional muscle denervation changes.

Acknowledgments The authors gratefully acknowledge Tim Phelps, Associate Professor and Medical Illustrator in the Department of Art as Applied to Medicine, The Johns Hopkins University, Baltimore, MD, for his great contribution in the illustration of the peroneal nerve.

References

1. Chhabra A, Williams EH, Wang KC, Dellon AL, Carrino JA. MR Neurography of neuromas related to nerve injury and entrapment with surgical correlation. AJNR Am J Neuroradiol. 2010;31:1363–8.
2. Thawait SK, Chaudhry V, Thawait GK, et al. High-resolution MR neurography of diffuse peripheral nerve lesions. AJNR Am J Neuroradiol. 2010 (EPUB).
3. Filler AG, Haynes J, Jordan SE, et al. Sciatica of nondisc origin and piriformis syndrome: diagnosis by magnetic resonance neurography and interventional magnetic resonance imaging with outcome study of resulting treatment. J Neurosurg Spine. 2005;2:99–115.
4. Filler A. Magnetic resonance neurography and diffusion tensor imaging: origins, history, and clinical impact of the first 50,000 cases with an assessment of efficacy and utility in a prospective 5,000-patient study group. Neurosurgery. 2009;65(4 Suppl):29–43.
5. Kim JY, Ihn YK, Kim JS, Chun KA, Sung MS, Cho KH. Non-traumatic peroneal nerve palsy: MRI findings. Clin Radiol. 2007;62(1):58–64.
6. Heilbrun ME, Tsuruda JS, Townsend JJ, Heilbrun MP. Intraneural perineurioma of the common peroneal nerve. Case report and review of the literature. J Neurosurg. 2001;94(5):811–5.
7. Hof JJ, Kliot M, Slimp J, Haynor DR. What's new in MRI of peripheral nerve entrapment? Neurosurg Clin N Am. 2008;19 (4):583–95.
8. Loredo R, Hodler J, Pedowitz R, Yeh LR, Trudell D, Resnick D. MRI of the common peroneal nerve: normal anatomy and evaluation of masses associated with nerve entrapment. J Comput Assist Tomogr. 1998;22(6):925–31.
9. Martinoli C, Bianchi S, Gandolfo N, Valle M, Simonetti S, Derchi LE. US of nerve entrapments in osteofibrous tunnels of the upper and lower limbs. Radiographics. 2000 Oct;20 Spec No:S199-213; discussion S213-7. Radiographics. 2000;20(6):1818.
10. Visser LH. High-resolution sonography of the common peroneal nerve: detection of intraneural ganglia. Neurology. 2006;67(8):1473–5.
11. Gruber H, Peer S, Meirer R, Bodner G. Peroneal nerve palsy associated with knee luxation: evaluation by sonography–initial experiences. AJR Am J Roentgenol. 2005;185(5):1119–25.
12. Hahn AF, Mauermann ML, Dyck PJ, Keegan BM. A 16-year-old girl with progressive weakness of the left leg. Neurology. 2007;69 (1):84–90.
13. McCrory P, Bell S, Bradshaw C. Nerve entrapments of the lower leg, ankle and foot in sport. Sports Med. 2002;32(6):371–91.
14. El Gharbawy RM, Skandalakis LJ, Skandalakis JE. Protective mechanisms of the common fibular nerve in and around the fibular tunnel: a new concept. Clin Anat. 2009;22(6):738–46.
15. Vieira RL, Rosenberg ZS, Kiprovski K. MRI of the distal biceps femoris muscle: normal anatomy, variants, and association with

common peroneal entrapment neuropathy. AJR Am J Roentgenol. 2007;189(3):549–55.
16. Fabre T, Piton C, Andre D, Lasseur E, Durandeau A. Peroneal nerve entrapment. J Bone Joint Surg Am. 1998;80(1):47–53.
17. Sunderland S, Bradley KC. The cross-sectional area of peripheral nerve trunks devoted to nerve fibers. Brain. 1949;72(3):428–49.
18. Aprile I, Caliandro P, La Torre G, Tonali P, Foschini M, Mondelli M, et al. Multicenter study of peroneal mononeuropathy: clinical, neurophysiologic, and quality of life assessment. J Peripher Nerv Syst. 2005;10(3):259–68.
19. Planner AC, Donaghy M, Moore NR. Causes of lumbosacral plexopathy. Clin Radiol. 2006;61:987–95.
20. Edwards Jr PH, Wright ML, Hartman JF. A practical approach for the differential diagnosis of chronic leg pain in the athlete. Am J Sports Med. 2005;33(8):1241.
21. McCrory P, Bell S, Bradshaw C. Nerve entrapment of the lower leg, ankle and foot in sport. Sports Med. 2002;32:371–91.
22. Bendszus M, Wessig C, et al. MR imaging in the differential diagnosis of neurogenic foot drop. AJNR Am J Neuroradiol. 2003;24:1283–9.
23. Masakado Y, Kawakami M, Suzuki K, Abe L, Ota T, Kimura A. Clinical neurophysiology in the diagnosis of peroneal nerve palsy. Keio J Med. 2008;57(2):84–9.
24. Kim S, Choi JY, Huh YM, et al. Role of magnetic resonance imaging in entrapment and compressive neuropathy - what, where, and how to see the peripheral nerves on the musculoskeletal magnetic resonance image: part 1. Overview and lower extremity. Eur Radiol. 2007;17:139–49.
25. Viallon M, Vargas MI, Jlassi H, Lovblad KO, Delavelle J. High-resolution and functional magnetic resonance imaging of the brachial plexus using an isotropic 3D T2 STIR (Short Term Inversion Recovery) SPACE sequence and diffusion tensor imaging. Eur Radiol. 2008;18:1018–23.
26. Zhang Z, Meng Q, Chen Y, et al. 3-T imaging of the cranial nerves using three-dimensional reversed FISP with diffusion-weighted MR sequence. J Magn Reson Imaging. 2008;27:454–8.
27. Stewart JD. Foot drop: where, why and what to do? Pract Neurol. 2008;8(3):158–69.
28. Erman T, Tuna M, Göçer AI, Idan F, Akgül E, Zorludemir S. Postoperative radicular neuroma. Case report. Neurosurg Focus. 2001 Nov 15;11(5).
29. Giannoudis PV, Kontakis G, Christoforakis Z, Akula M, Tosounidis T, Koutras C. Management, complications and clinical results of femoral head fractures. Injury. 2009;40 (12):1245–51.
30. Montgomery AS, Birch R, Malone A. Entrapment of a displaced common peroneal nerve following knee ligament reconstruction. J Bone Joint Surg Br. 2005 Jun;87(6):861–2. Erratum in: J Bone Joint Surg Br. 2005;87(8):1166.
31. Ottomley N, Williams A, Birch R, Noorani A, Lewis A, Lavelle J. Displacement of the common peroneal nerve in posterolateral corner injuries of the knee. J Bone Joint Surg Br. 2005;87 (9):1225–6.
32. Williams EH, Williams CG, Rosson GD, Dellon AL. Combined peroneal and proximal tibial nerve palsies. Microsurgery. 2009;29 (4):259–64.
33. Canella C, Demondion X, Guillin R, Boutry N, Peltier J, Cotton A. Anatomic study of the superficial peroneal nerve using sonography. AJR AM J Roentgenol. 2009;193(1):174–9.
34. Garozzo D, Ferraresi S, Buffatti P. Surgical treatment of common peroneal nerve injuries: indications and results. A series of 62 cases. J Neurosurg Sci. 2004;48(3):105–1.
35. Cardelia JM, Dormans JP, Drummond DS, Davidson RS, Duhaime C, Sutton L. Proximal fibular osteochondroma with associated peroneal nerve palsy: a review of six cases. J Pediatr Orthop. 1995;15(5):574–7.
36. Elias WJ, Pouratian N, Oskouian RJ, Schirmer B, Burns T. Peroneal neuropathy following successful bariatric surgery. Case report and review of the literature. J Neurosurg. 2006;105(4):631–5.
37. Spinner RJ, Amrami KK, Wolanskyj AP, Desy NM, Wang H, Benarroch EE, et al. Dynamic phases of peroneal and tibial intraneural ganglia formation: a new dimension added to the unifying articular theory. J Neurosurg. 2007;107:296–307.
38. Peeters EY, Neiboer KH, Osteaux MM. Sonography of the normal ulnar nerve at Guyon's canal and of the common peroneal nerve dorsal to the fibular head. J Clin Ultrasound. 2004;32(8):375–80.
39. Spinner RJ, Desy NM, Amrami KK. Sequential tibial and peroneal intraneural ganglia arising from the superior tibiofibular joint. Skeletal Radiol. 2008;37(1):79–84.
40. Descamps MJ, Barrett L, Groves M, Yung L, Birch R, Murray NM, et al. Primary sciatic nerve lymphoma: a case report and review of the literature. J Neurol Neurosurg Psychiatry. 2006;77 (9):1087–9.
41. Mahitchi E, Van Linthoudt D. Schwannoma of the deep peroneal nerve. An unusual presentation in rheumatology. Praxis (Bern 1994). 2007;96(3):69–72.
42. Ladha SS, Dyck PJ, Spinner RJ, Perez DG, Zeldenrust SR, Amrami KK, et al. Isolated amyloidosis presenting with lumbosacral radiculoplexopathy: description of two cases and pathogenic review. J Peripher Nerv Syst. 2006;11(4):346–52.
43. Linssen WH, Steller EP, Spliet WG, Davies GA. Peroneal nerve compression by fibrous histiocytoma. J Neurol. 2000;247(1):68–9.
44. Nagel A, Greenebaum E, Singson RD, Rosenwasser MP, McCann PD. Foot drop in a long-distance runner. An unusual presentation of neurofibromatosis. Orthop Rev. 1994;23(6):526–30.
45. Trăistaru R, Enăchescu V, Manuc D, Gruia C, Ghiluşi M. Multiple right schwannoma. Rom J Morphol Embryol. 2008;49 (2):235–9.
46. Yamamoto T, Maruyama S, Mizuno K. Schwannomatosis of the sciatic nerve. Skeletal Radiol. 2001;30(2):109–13.
47. Hruban RH, Shiu MH, Senie RT, Woodruff JM. Malignant peripheral nerve sheath tumors of the buttock and lower extremity. A study of 43 cases. Cancer. 1990;66:1253–65.
48. Yamashita T, Kwee TC, Takahara T. Whole-body magnetic resonance neurography. N Engl J Med. 2009;361(5):538–9.
49. Jebraj I, Rao A, Shyamkumar NK, Vidyasagar. Imaging of tender neuropathy in leprosy. Indian J Lepr. 2005;77(1):51–4.
50. Hanyu N, Ikeda S, Nakadai A, Yanagisawa N, Powell HC. Peripheral nerve pathological findings in familial amyloid polyneuropathy: a correlative study of proximal sciatic nerve and sural nerve lesions. Ann Neurol. 1989;25(4):340–50.
51. Pradat PF, Bouche P, Delanian S. Sciatic nerve moneuropathy: an unusual late effect of radiotherapy. Muscle Nerve. 2009;40 (5):872–4.
52. Paulino AC. Late effects of radiotherapy for pediatric extremity sarcomas. Int J Radiat Oncol Biol Phys. 2004;60 (1):265–74.
53. Emami B, Lyman J, Brown A, Coia L, Goitein M, Munzenrider JE, et al. Tolerance of normal tissue to therapeutic irradiation. Int J Radiat Oncol Biol Phys. 1991;21:109–22.
54. Kumar RS, Gopinath M. A rare cause of foot drop after radiofrequency ablation for varicose veins: case report and review of the literature. Neurol India. 2010;58(2):303–5.
55. Andreisek G, Nanz D, Weishaupt D, Pfammatter T. MR imaging–guided percutaneous sclerotherapy of peripheral venous malformations with a clinical 1.5-T unit: a pilot study. J Vasc Interv Radiol. 2009;20(7):879–87.